frontiers | Frontiers in Mechanical Engineering

TYPE Original Research
PUBLISHED 17 April 2024
DOI 10.3389/fmech.2024.1351922

OPEN ACCESS

EDITED BY
Hamid Reza Karimi,
Polytechnic University of Milan, Italy

REVIEWED BY
Gürel Çam,
Iskenderun Technical University, Türkiye
Yanfeng Peng,
Hunan University of Science and Engineering, China

*CORRESPONDENCE
Hua Mu,
Ym197920060516@163.com

RECEIVED 07 December 2023
ACCEPTED 28 March 2024
PUBLISHED 17 April 2024

CITATION
Ni X, Xu S and Mu H (2024), Effect of Mn-content of ER5356 welding rods on mechanical properties of Al-alloys joints.
Front. Mech. Eng 10:1351922.
doi: 10.3389/fmech.2024.1351922

Effect of Mn-content of ER5356 welding rods on mechanical properties of Al-alloys joints

Xianpeng Ni[1], Shaohua Xu[1] and Hua Mu[2]*

[1]School of Mechanical and Electrical Engineering, Shandong Vocational College of Industry, Zibo, China, [2]Science and Technology Report Center, Shandong Institute of Scientific and Technical Information, Jinan, China

Introduction: Compared with imported welding wire, domestic aluminum alloy welding wire has more internal inclusion defects. To improve the welding quality and reliability of aluminum alloy, the welding performance of aluminum alloy was improved by adding different content of Mn element.

Methods: ER5356 aluminum alloy ingot with different Mn content (0.05% and 0.15%) was prepared by semi-continuous casting and gravity casting. After stretching, the mechanical properties and microstructure of ER5356 aluminum alloy were studied. In addition, the microstructure, microhardness and mechanical behavior of ER5356 aluminum alloy welding wire with 6082 and 7005 aluminum alloy joints were studied.

Results and Discussion: Compared with gravity casting, the yield strength and tensile strength of ER5356 (0.15% Mn) were increased by 12.8% and 3.17% respectively. The head influence zone of the joint made of metal wire containing 0.15% Mn is slightly wider than that of the joint made of ER535 (0.05% Mn) containing 0.05% Mn. The quality of ER5356 aluminum alloy welding wire blocked by semi-continuous casting is better than that of ER5356 aluminum alloy welding wire blocked by gravity casting method. Mn element can improve the metal deposition process in welding.

Conclusion: The research method can improve the welding current control and welding quality, and has important practical significance in improving the mechanical properties of welding seams.

KEYWORDS

ER5356, Mn content, welding wire structure, welding mechanics, deposition technology

1 Introduction

Welding technology is a crucial method of joining materials in modern industrial production. It is widely utilized in fields such as aerospace, automobile manufacturing, and power equipment (Qu et al., 2021; Nafeez et al., 2022). Several welding techniques are utilized for welding Al-alloys in these applications, including laser beam welding (Kim et al., 2023; Cam and Ipekoglu, 2017; Kashaev et al., 2018), friction stir welding (Kucukomeroglu et al., 2019; Ahmed et al., 2023a; Ahmed et al., 2023b; Cam et al., 2023; Khaliq et al., 2023), and conventional arc welding methods (Ipekoglu and Cam, 2019). As the case in steels (Serindag et al., 2022; Senol and Cam, 2023; Serindag and Cam, 2023), gas tungsten arc welding (GTAW), also known as TIG

welding, and gas metal arc welding (GMAW), also referred to as MIG/MAG welding, are widely used in welding Al-alloys with filler rods. However, the mechanical property (MP) of ER5356 welding strip (ER5356-WS) is strongly associated with the welding wire structure (WWS). Nevertheless, there is a noticeable shortage of relevant research in this area. To address this gap and optimize the performance of ER5356-WS, studies have been conducted to reveal the effect of Mn on the MP and WWS of ER5356-WS by adding Mn element. The element manganese, being a frequent component of aluminum alloys, significantly impacts the properties of said alloys. Nonetheless, its contribution to ER5356-WS remains insufficiently studied. Therefore, the study's objective is to examine how Mn elements impact the properties of ER5356-WS by conducting MP and WWS on Mn-incorporated ER5356-WS. To achieve this, standard MP tests and microstructural observation methods were utilized for a comprehensive analysis of Mn-incorporated ER5356-WS. The study utilized the MP test to determine the hardness, strength, and toughness, followed by microstructure observation to conduct an in-depth analysis of the organizational structure. The study's innovation lies in the incorporation of Mn into ER5356-WS, providing insights into the effect of this element on the MP and WWS. This discovery offers a new approach to optimizing the performance of ER5356-WS. The study's findings contribute to the existing knowledge in the field of welding mechanics and deposition technology by providing a detailed analysis of how manganese content affects the mechanical properties of an ER5356 alloy during the welding process. Insights into the role of Mn have led to a better understanding of its impact on microhardness, tensile strength, and fracture morphology. The study shows that higher Mn content, specifically 0.15%, has a positive effect on the yield strength and tensile strength of welded joints. Additionally, the research provides new insights into the heat-affected zone (HAZ), revealing that an increase in Mn content results in a broader HAZ, which is crucial for assessing weld quality. The study also explains how welding current and Mn content interact to affect the weld formation and metal deposition process. The control of these factors can greatly improve welding quality. This makes the conclusions of the study not only theoretically valuable but also practically applicable in industrial settings where precise welding is essential. The study will be conducted in four sections. The first section provides an overview of the mechanical properties and weldability of ER5356-WS with added Mn. The second section analyzes the mechanical properties and weldability of ER5356-WS with added Mn. In the third section, the study experimentally validate the findings from the second section. Finally, the fourth section summarizes the study's results and highlights any limitations.

2 Related works

ER5356-WS is a crucial welding material for aluminum alloys, and its application performance is significantly affected by its MP and WWS. Senthur Vaishnavan and Jayakumar raised the issue of scandium in aluminum alloy mixtures significantly improved the welding of aluminum alloys showing enhancement in strength and hardness of welded joints. The GTAW welded joints with scandium addition showed enhanced yield strength and hardness enhancement up to 124 HV.1 The results of the study showed that scandium had an important role in aluminum alloy welding (Salah et al., 2022). Kamoon et al. based on the fact that AA6061-T6 alloy was sensitive during heat treatment and the microstructure would be affected during welding. The HAZ microstructure of welded samples at different temperatures was evaluated. The results showed that AA6061-T6 recovered its microstructure and hardness by post-weld heat treatment, while the filler metal -ER5356- remained unchanged. The post-weld heat treatment increased the hardness of the alloy from 60 HV to 80 HV (Haryadi et al., 2020). Sokoluk's research team found that by introducing nanoparticle-enabled phase control during the welding process, 7,075 can be safely arc welded without thermal cracking. Joints welded with 7,075 filled rods containing TiC nanoparticles exhibited excellent tensile strength and improved second phase, eliminating thermal crack susceptibility, and this simple torsion method can be applied to a wide range of thermal crack sensitive materials (Baskoro et al., 2020). Mehdi and Mishra investigated the effect of friction stir treatment on GTAW welded joints filled with ER 5356 to improve the MP of GTAW welded joints. By adjusting the process parameters of friction stir welding, the FSP tool pin was rotated on the welded joints in order to reduce the weld loads and improve the quality of the weld. The results showed that the minimum compressive residual stress of 18 MPa, the maximum tensile strength of 281.1 MPa and the hardness of 107 HV were located in the molten core region of the GTAW + FSP weldment. The predicted peak temperature in the weld region was calculated and the maximum temperature (505°C) and maximum heat flux (2.93 × 10(6) w/m(2)) were observed at a tool speed of 1,300 rpm (Samiuddin et al., 2021). Naing and Muangjunburee evaluated the effect of two alternative fillers, ER 4043 and ER 5356, on the metallurgical and mechanical properties of welded joints in MIG weld repair of 6082-T6 aluminum alloy. The results showed that the tensile and yield strengths of welded joints with ER 4043 filler decreased, while the tensile and yield strengths of welded joints with ER 5356 filler remained unchanged. The tensile strength of ER 5356 braze filler welded joints was higher than that of ER 4043 braze, indicating that ER 5356 braze should be preferentially used for filler welding of 6082-T6 aluminum alloy (Senthur Vaishnavan and Jayakumar, 2021).

The significant function of manganese in aluminum alloys has stimulated investigations of its function in ER5356-WS. The findings will establish a crucial theoretical foundation for refining the performance of ER5356-WS. Qi et al. investigated the MP and microstructural evolution of single-crystal face-centered cubic cobalt-nickel-based high-entropy alloys using molecular dynamics simulations. The results showed that the addition of copper and manganese elements decreased the lamellar dislocation energy, leading to dislocation-mediated deformation. Cobalt-chromium-nickel-copper HEA showed the highest indentation force, followed by cobalt-chromium-nickel and cobalt-chromium-nickel-manganese-hafnium. Cu and Mn elements favor amorphization, while the addition of Cu resulted in irregular slip patterns accompanied by dislocation rings (Khan et al., 2021). Abhijit et al. realized two-phase microstructures including complex solid solution phases, dislocations and nano-twins in CoCrFeMnNi system. High hardness of 6.3 GPa and negative strain rate sensitivity of - 0.0206 were observed. Various interactions between dislocations and grain/interface/twin boundaries were responsible for the observed flow characteristics. The results

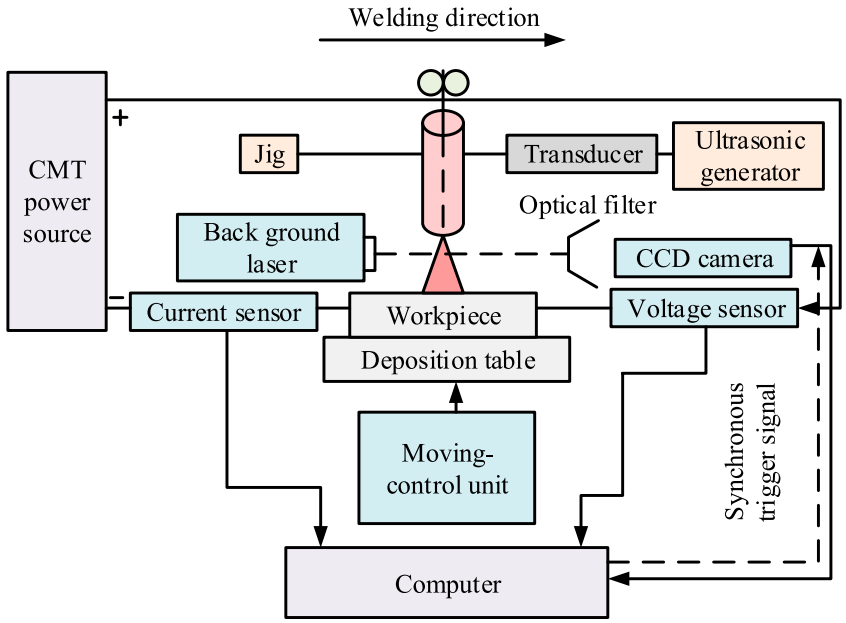

FIGURE 1
Schematic diagram of experimental deposition system.

showed that dislocation-solute atom interactions were not working in this alloy system (Sokoluk et al., 2019). Peng et al. obtained four different types of Mn presence in Mg-2.0Zn-1.5Mn magnesium alloy by different heat treatments. The results showed that the preexisting nanoscale α-Mn particles had a good pinning effect on refining the grains. The micrometer-scale α-Mn phase activated the particle-excited nucleation mechanism. The combination of micron-sized α-Mn phase + nanosized α-Mn phase showed the best grain refinement, with tensile yield strength, tensile strength and elongation at break of 267 MPa, 305 MPa and 28.6%, respectively, and MP was significantly improved (Mehdi and Mishra, 2020).

In summary, incorporating Mn into ER5356-WS can greatly improve its melting point and wetting and spreading behavior. This advancement not only presents a novel approach to enhancing ER5356-WS properties, but also establishes a theoretical foundation for Mn's application as a welding material element in aluminum alloys. Nevertheless, effectively controlling and integrating the addition of Mn into ER5356-WS remains a major obstacle that necessitates further investigation.

3 Preparation studies of MP and WWS of ER5356-WS incorporated with Mn

The study focuses on an in-depth analysis of the compositional design and extrusion-drawing of ER5356 aluminum alloy (ER5356-AA), and further explores the change in WWS after drawing of welded bars. The focus of the study was then shifted to the effect of incorporating Mn elements on the change of ER5356-WSWS. It is expected to provide an important basis for the physical property changes of ER5356-AA welded bars, as well as a new theoretical perspective on WWS optimization.

3.1 ER5356 aluminum alloy composition design and extrusion and drawing research

In the first phase of the ER5356-WWS preparation study, the first task was to understand the compositional design of the ER5356-AA and the effects of its extrusion and drawing process (Qi et al., 2021; Naing and Muangjunburee, 2022). This phase of the study provided the basis for subsequent welding bar preparation and WWS analysis. In particular, the compositional design of ER5356-AA has a significant influence on its MP and WWS, while the extrusion and drawing process directly determines the microstructure and properties of the welded bars.

Aluminum alloy ingot casting is an important link in the production of welding wire, and the national standard GB/T 10,858-2012 Aluminum and Aluminum Alloy Welding Wire stipulates the alloy composition of welding wire. Considering the existence of burnout of Mg element in the melting process, ER5356-AA with different Mn content was studied and designed. The ordinary gravity casting method was adopted, and the raw materials were selected as 99.9% purity Al and Mg ingots and 10% purity Mn, Ti and Cr alloying additives for refining and casting (Abhijit et al., 2019; Peng et al., 2022). Schematic diagram of the experimental deposition system is shown in Figure 1.

In Figure 1, the experimental system consists of three parts: the deposition system, the electrical parameter acquisition system and the image acquisition system. The deposition system is responsible for implementing the deposition experiment under each parameter to provide samples. The electrical parameter acquisition system is used to collect parameters such as current and voltage during the deposition process; and the image acquisition system is responsible for photographing the transition of the droplets and the melt pool morphology during the deposition process. The extruder and drawer were used for the test, as shown in Figure 2.

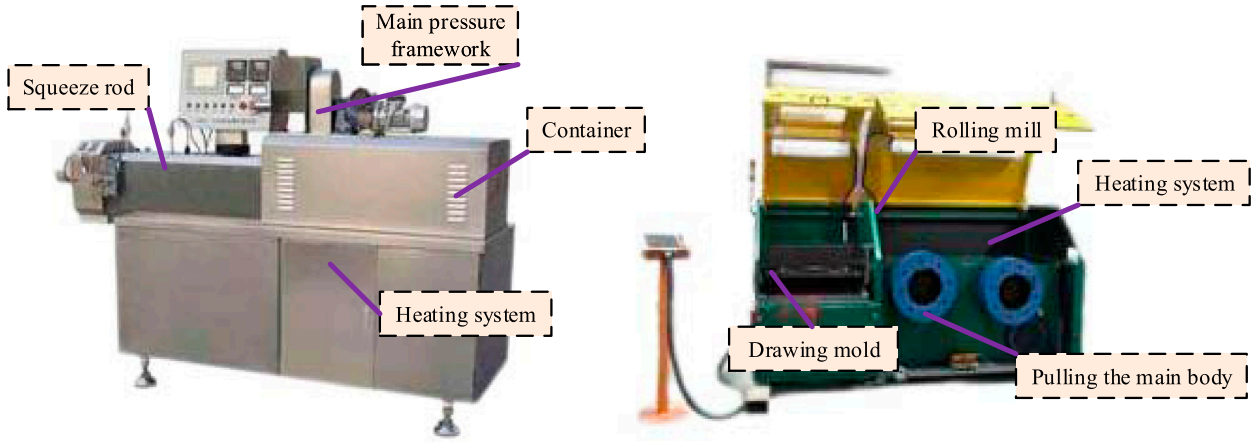

FIGURE 2
Extruder and drawing machine for testing.

In Figure 2, after melting of ER5356-AA, extrusion and drawing processes are required. Extrusion equipment includes an extruder and an industrial heat treatment furnace. Prior to extrusion, it is necessary to heat and insulate the aluminum alloy ingot to prevent the metal from melting due to excessively high temperatures or extrusion difficulties due to excessively low temperatures. The holding temperature is set at 500°C and the holding time is 3 h. The drawing process requires equipment such as drawing machines, industrial heat treatment furnaces and rolling mills. Before drawing, the front end of the extrusion rod needs to be processed using a rolling mill to ensure that it can pass through the die smoothly, and the extrusion rod is coated with lubricating oil to prevent damage to the die and ensure that the drawing is smooth. During the drawing process, an intermediate annealing treatment is required.

Microhardness is an important measure of the ability of a metallic material to resist hard objects pressed into its surface, and can reflect the local mechanical properties of the material. Specifically, the greater the resistance of the material, the higher the hardness, and *vice versa*, the lower. Commonly used microhardness testing indicators include Brinell hardness, Rockwell hardness, Vickers hardness and microhardness. Microhardness testing is a common means of determining the quality of materials, including the detection of wire drawing rods and welded joints (Kim et al., 2021; Fang et al., 2022). Standard tensile specimens were prepared and dimensionally measured. A manual GTAW method, also known as TIG, was used to weld 6,082 and 7,005 aluminum alloys using ER5356 filler rods with varying Mn-contents. The welding was carried out under the shielding gas of pure argon supplied at a flow rate of 14 L/min, using a WSE-500 AC/DC pulsed square-wave GTAW welding machine. The rationality of the joint design closely relates to the strength and performance of the welded joints. Therefore, weld grooves were prepared on the plates to be welded. The first step was to clean the surface of the base metal and filler wire to be welded, removing any oil and oxide film. The heat input, which is the energy transferred to the joint during the welding process, has a significant effect on the metallurgical and mechanical characteristics of the produced joints. Too small a heat input leads to defects such as under-welding and holes, while too large a heat input

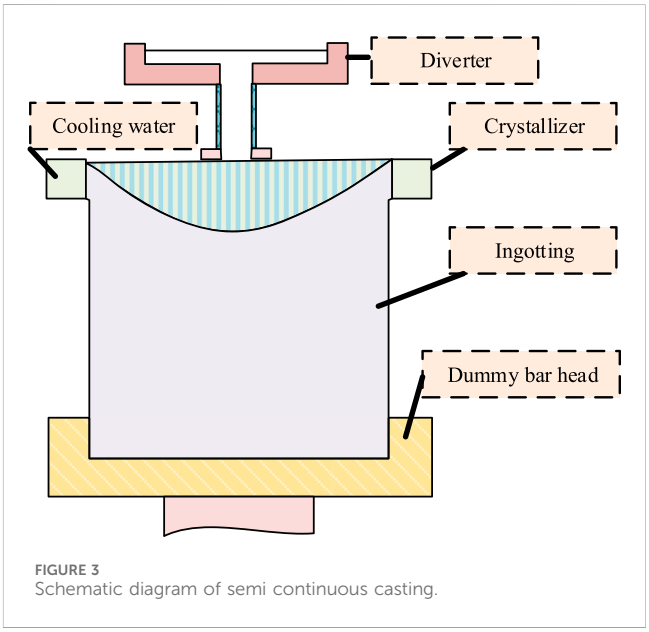

FIGURE 3
Schematic diagram of semi continuous casting.

affects the forming quality of the joint surface and increases the grain size in the weld zone. The welding heat input is shown in Eq. 1.

$$Q = \frac{UI\eta \times 60}{v \times 10^3} \quad (1)$$

In Eq. 1, Q is the welding heat input per unit length, U is the welding voltage, I is the welding current, η is the welding thermal efficiency, and v is the welding speed.

3.2 Study on the preparation of WWS after drawing of ER5356-WS

After examining the ER5356-AA's composition, design, and extrusion and drawing processes, the study's focus turned to preparing ER5356-WWS after drawing. This transition naturally

leads to the next step of investigating how to prepare WWS welding rods after drawing on the basis of the previously designed, extruded, and drawn aluminum alloy. Aluminum alloy ingots utilized for ER5356-AA wires present a range of issues, including excessive oxidation inclusions, coarse grain size, unstable quality, and constituent segregation. These problems considerably hamper the wire's quality and render it challenging to meet the need for first-rate welding, particularly in the aerospace, military, high-speed train, and other related industries. Figure 3 displays the semi-continuous casting principle diagram.

In Figure 3, the main technologies for producing aluminum alloy ingots are continuous casting and semi-continuous casting technology. Semi-continuous casting technology is a more appropriate choice for producing aluminum alloy ingots with lower cost, high quality requirements, and wide product specifications. This is because continuous casting technology has limited ingot specifications, resulting in single product and poor flexibility. According to the molding direction of the ingot, semi-continuous casting can be divided into vertical casting and horizontal casting, of which vertical semi-continuous casting method is suitable for more aluminum alloy components and a variety of casting specifications. Aluminum alloy ingots obtained from casting need to be homogenized and heat-treated, and enter the extrusion process, and the subsequent heat preservation treatment and extrusion conditions also have a direct impact on product quality (Mercan et al., 2020; Çömez and Durmuş, 2020).

General aluminum alloy drawing channel deformation rate between 20% and 60%, too large easily lead to pull off, broken, need to be in the wire drawing before the channel calculation. The process needs to be prevented from pulling or even pulling off due to deformation resistance is too large, the channel deformation rate needs to be controlled at about 20%, with the increase in the number of pulling channel, wire diameter decreases, channel deformation rate should also be reduced accordingly. Drawing channel as shown in Eq. 2.

$$n = \frac{\ln \lambda_\varepsilon}{\ln \lambda_m} \tag{2}$$

In Eq. 2, n is the number of drawing passes, λ_ε is the total elongation factor, and λ_m is the average elongation factor. The elongation factor is shown in Eq. 3.

$$\lambda = \frac{{D_q}^2}{{D_H}^2} \tag{3}$$

In Eq. 3, D_q is the diameter before drawing and D_H is the final diameter of drawing. The elongation is shown in Eq. 4.

$$\delta = \left[\left(\frac{d_\theta}{d_K}\right)^2 - 1\right] \times 100\% \tag{4}$$

In Eq. 4, δ is the elongation and the relationship between δ and λ is shown in Eq. 5.

$$\delta = (\lambda - 1) \times 100\% \tag{5}$$

The average tensile strength is shown in Eq. 6.

$$\sigma_{bicp} = \frac{\sigma_{b(i-1)} + \sigma_{bi}}{2} = \frac{2\sigma_{bo} + \sum_1^i \Delta\sigma_{bi}}{2} \tag{6}$$

In Eq. 6, σ_{bicp} denotes average compressive strength, $\sigma_{b(i-1)}$ denotes pre-drawing tensile strength, σ_{bi} denotes post-drawing tensile strength, and σ_{bo} is the initial pre-drawing tensile strength. $\Delta\sigma_{bi}$ is the post-drawing tensile strength increment, and $i_1\Delta\sigma_{bi}$ is the post-drawing cumulative tensile strength increment. The through compression ratio is shown in Eq. 7.

$$\begin{cases} q_i = \dfrac{d_{i-1}^2 - d_i^2}{d_{i-1}^2} \\ d_i^2 = (1-q)d_{i-1}^2 \end{cases} \tag{7}$$

In Eq. 7, d_i is the diameter of aluminum wire after drawing of the process, and q_i is the compression rate of the process. Welding wire drawing process, as shown in Figure 4.

In Figure 4, the drawing quality is affected by drawing speed, lubrication conditions and mold condition. Appropriate drawing speed can avoid stress concentration and pull-off phenomenon, and improve production efficiency. Lubricant can reduce the direct contact between the wire blank and the mold, prolonging the life of the mold and reducing mold scratches. However, the mold will wear out over time and with use, and requires regular cleaning and maintenance. During the drawing process, the material undergoes plastic deformation, which increases dislocation density, work hardening, and residual stresses. In order to solve these problems, wire blanks need to be intermediate annealing treatment to eliminate work hardening and residual stress. The annealing time should not be too long, in order to prevent excessive grain size leading to softening and pull-off phenomenon.

3.3 Preparation of Mn-incorporated ER5356-WS for WWS studies

In order to further optimize the WWS of ER5356-WS, the study employed the incorporation of Mn into the welding rod. First, the amount of Mn added was determined. Under the premise of ensuring the basic performance of the welding wire, the optimal amount of Mn addition was searched for, so that the welding wire could obtain better strength and plasticity during the welding process. Then, the melting process was optimized. During the melting process, the dissolution and distribution of Mn were controlled by adjusting the furnace temperature and holding time to further optimize the organization of the wire. Finally, the subsequent heat treatment was carried out. By adjusting the solid solution temperature and aging treatment parameters, the best matching of the organization and properties of the welding wire was achieved (Waziri and Ibrahim, 2022; Yılmaz and Fındık, 2022).

During the preparation process, special treatments were carried out for the characteristics of 6,082 and 7,005 aluminum alloys. Considering that these two aluminum alloys have excellent welding forming and corrosion resistance, suitable operation methods are adopted during melting and heat treatment to ensure the stable performance of the wires. By choosing the sinusoidal function to model a single pass, it was found that the lap spacing directly affects the surface quality of single-layer multi-

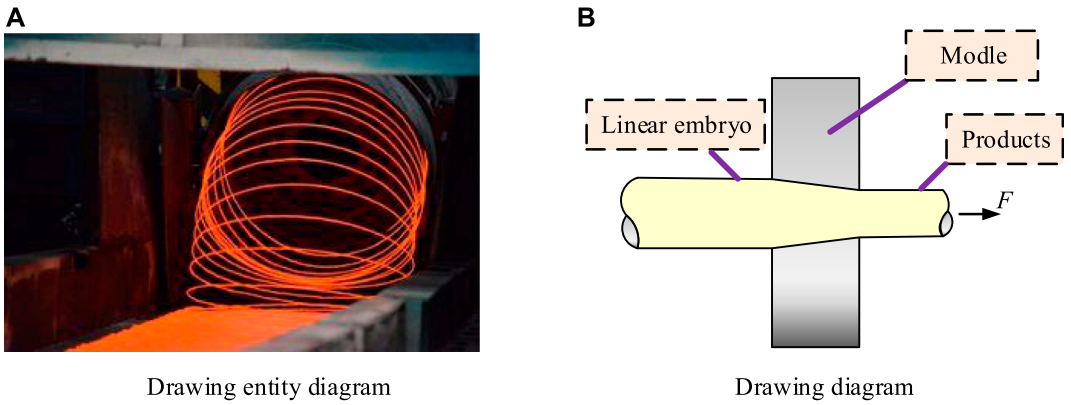

FIGURE 4
Welding wire drawing process. **(A)** Drawing entity diagram. **(B)** Drawing diagram.

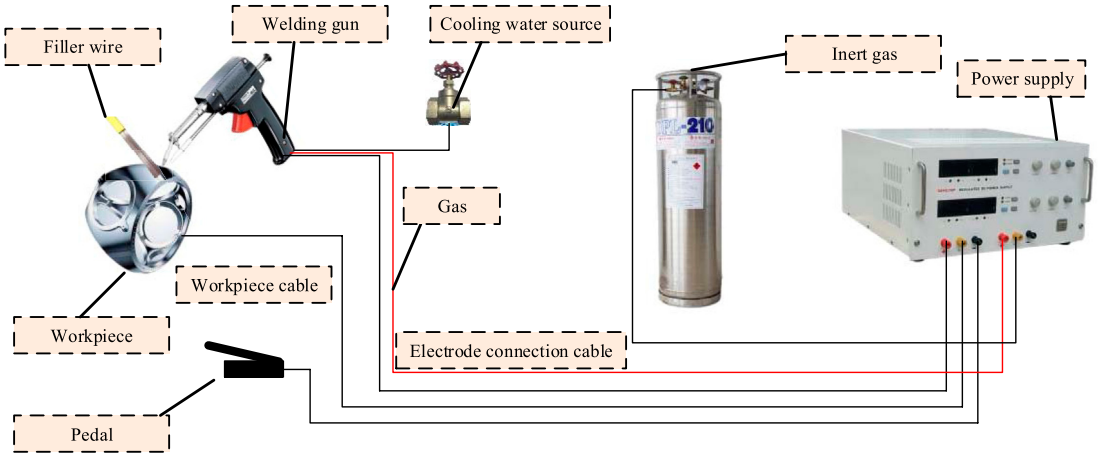

FIGURE 5
GTAW welding circuit diagram.

pass molding. When the spacing is too large, there is no overlap, and when it is too small, there is underlap, and the ideal overlap is that the overlap area of the welded channel is equal to the area of the valley. Continuing to reduce the spacing will result in the formation of wave crests, destroying the surface flatness. The lap spacing can be determined according to the single-layer single-pass morphology curve, and there is no need to repeat the test when the corresponding process parameters are changed. There are two ideal lap models, the flat-top model and the sloping-top model. According to the flat-top model, the ideal lap spacing condition is that the area of the overlap region and the area of the trough region are equal. The profile curve of the first single pass is shown in Eq. 8.

$$f(x) = h\sin(\pi x/w) \tag{8}$$

In Eq. 8, h is the height of the apex of a single channel and w is the channel width of a single channel. The sloping top lap model suggests that the liquid metal fills unevenly in the trough region and the free surface cannot form a plane during solidification. The curved edge triangle is shown in Eq. 9.

$$S_{AFB} = \int_d^w f(x)dx = \frac{wh}{\pi}\left[\cos\left(\frac{wd}{\pi}\right) + 1\right] \tag{9}$$

In Eq. 9, A is the lap spacing and AA is the area of the curved triangle. The choice of this welding lap model has a direct influence on the microstructure and performance of the welded joint. In the welding process, GTAW method was used. Utilizing the characteristics of GTAW welding, i.e., stable welding process, easy to operate, good protection, and low economic cost, the quality of the welded joints was ensured. GTAW Welding Circuit Diagram, as shown in Figure 5.

In Figure 5, the welded joint consists of Weld Zone, HAZ and Parent Material (PM), and the microstructure and properties of each zone are the result of the combined influence of various factors during the welding process. The weld zone is the core part of the welded joint, which is formed by melting the two parts and then cooling and solidifying them. During the welding process, the microstructural evolution and properties of the weld zone are affected by various factors, including the distribution of alloying elements, the shape and size of the grains, and the rate of melting and solidification. The HAZ is the area around the weld zone that is

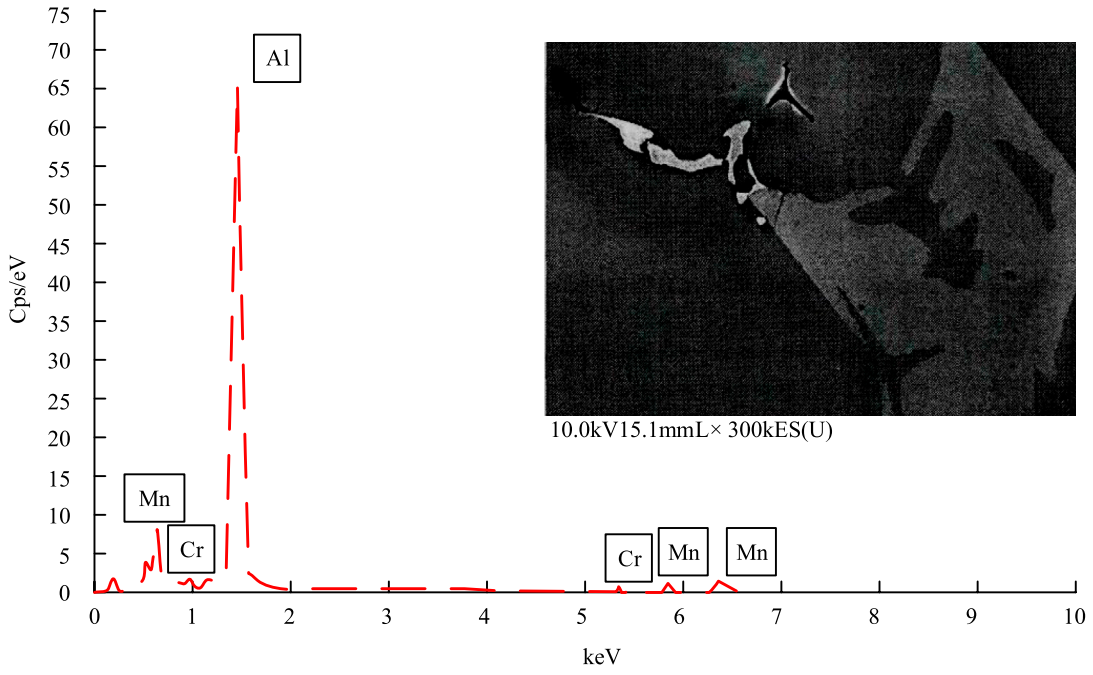

FIGURE 6
Energy spectrum analysis of homogenized microstructure of ER5356 aluminum alloy.

affected by the heat input of the weld. In this zone, although the material does not reach the melting temperature, the microstructure and properties of the material change due to the thermal influence of high temperature. According to the degree of heat influence, HAZ can be subdivided into fully austenitic zone, partially austenitic zone and undeformed austenitic zone, and the properties of these different zones will be different. PM refers to the non-melting region of the welded joint, i.e., the part that is not affected by the heat of welding. During the welding process, the organizational structure and properties of the PM remain essentially unchanged because it is not affected by the high temperature.

4 MP and WWS analysis of ER5356-WS incorporating Mn

The properties and microhardness of the semi-continuous cast aluminum alloy used for ER5356 will be studied in detail in the expectation of understanding the effect of Mn element on the properties of the aluminum alloy. The objective of this study is to reveal the effect of Mn on the properties of welded joints. To achieve this, the properties of welded joints produced from ER5356 filler rods with and without Mn will be compared.

4.1 Analysis of compressive organization and tensile properties of ER5356 aluminum alloy

The compressive organization and tensile properties of ER5356-AA are important indicators of its mechanical properties. Due to the wide application of ER5356-AA in various industrial fields, in-depth understanding of its MP will play an important role in optimizing its practical application. Therefore, the main work of this subsection is to provide a detailed analysis of its compressive organization and tensile properties. Immediately after that, the homogenized organization of ER5356-AA will be subjected to energy spectrum analysis and the detailed results are shown in Figure 6.

In Figure 6, the results of the energy spectrum analysis of the homogenized organization of semi-continuous cast ER5356-AA (0.15% Mn) are presented. This result reveals that the aluminum-manganese (Al-Mn) diffuse phase does not disappear with the as-cast organization despite the homogenization treatment. The size of the Al-Mn dispersed phase after homogenization treatment was reduced compared to the Al-Mn dispersed phase in the as-cast tissue. The extruded tissue characteristics of ER5356-AA, as shown in Figure 7.

In Figure 7, the metallographic organization of ER5356 (0.15% Mn) aluminum alloy after extrusion treatment is shown. The extrusion process resulted in the fragmentation of grains and disappearance of grain boundaries, while more fine diffuse phases were generated. This is mainly attributed to the extrusion and rupture of grains along the pressure direction during the extrusion process. In addition, more extrusion defects appeared inside the extrusion-treated samples, which had an impact on the material properties. For ER5356 (0.15% Mn), its organization after semi-continuous casting and gravity casting is shown in Fig. 3.6(d) and 3.6(c). The addition of manganese (Mn) to the ER5356 welding rod significantly influences the casting structure. When Mn is added, particularly at a level of 0.15%, the as-cast microstructure of ER5356 undergoes a notable change, with the primary aluminum phase becoming finer and more evenly distributed. The addition of Mn results in the formation of fine, dispersed Al-Mn particles throughout the cast alloy, which act as nucleation sites during solidification, thus refining the overall casting structure.

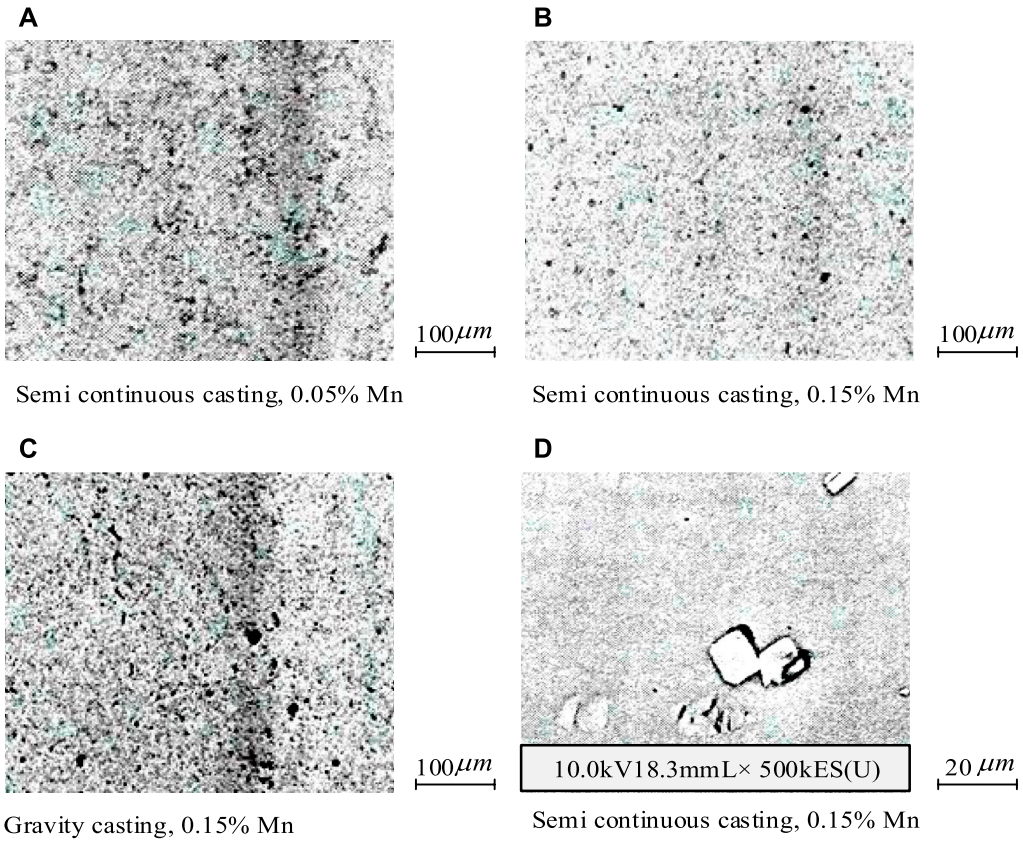

FIGURE 7
Microstructure characteristics of ER5356 aluminum alloy during extrusion. **(A)** Semi continuous casting, 0.05% Mn. **(B)** Semi continuous casting, 0.15% Mn. **(C)** Gravity casting, 0.15% Mn. **(D)** Semi continuous casting, 0.15% Mn.

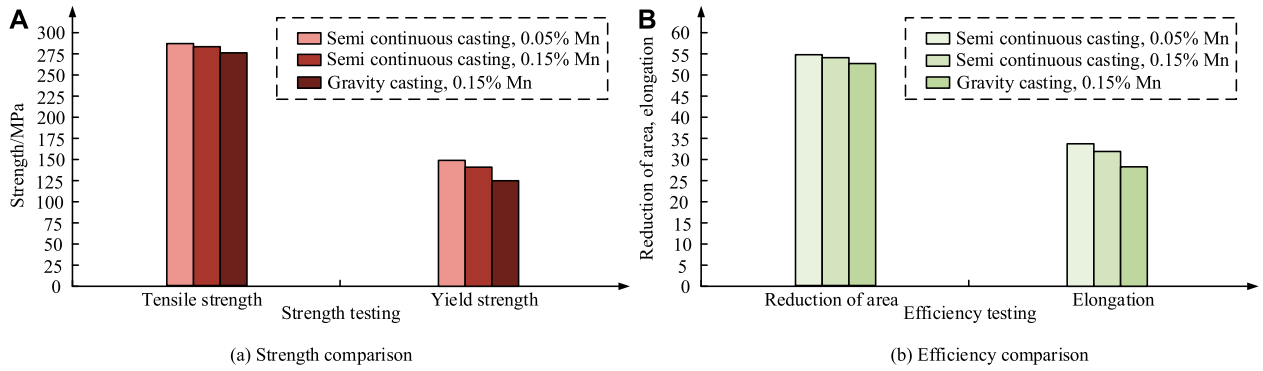

FIGURE 8
Mechanical properties of extrusion rod. **(A)** Strength comparison. **(B)** Efficiency comparison.

Additionally, Mn-rich particles contribute to enhancing strength by impeding dislocation movement within the aluminum matrix. This change is crucial in improving mechanical properties, such as tensile and yield strength, as shown in Fig. 3.6(c) and (d). MP of the extruded rod, as shown in Figure 8.

In Figure 8, tensile test MP data for three sets of 9.5 mm diameter specimens in the extruded state are demonstrated. The MP of semi-continuously cast ER5356-AA after extrusion is significantly better than that of the similar aluminum alloy obtained from gravity casting. In particular, the tensile and yield strengths, as well as the elongation at break and section shrinkage, are significantly improved. The MP of semi-continuously cast ER5356 (0.15% Mn) is slightly better than that of the gravity cast one, even when the compositions are the same. And the tensile strength and yield strength of semi-continuous cast ER5356 (0.05% Mn) specimens can be improved by 3.17% and 12.8% compared to gravity cast ER5356 (0.15% Mn).

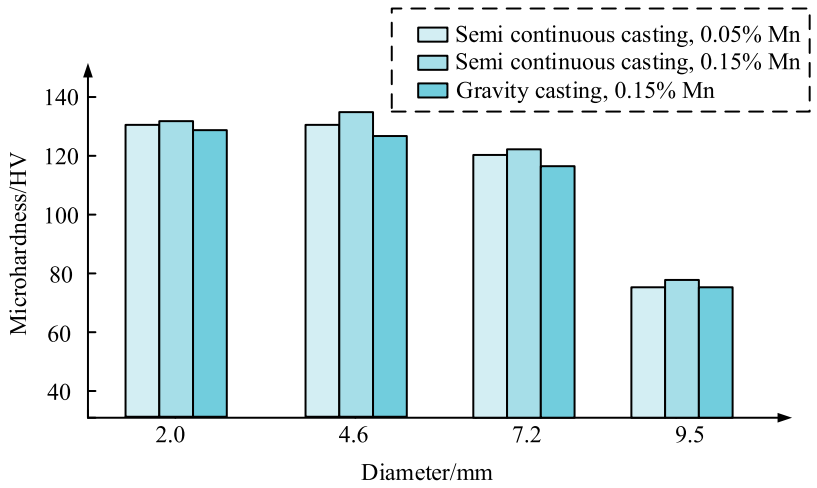

FIGURE 9
Gravity casting ER5356 (0.15% Mn) microhardness.

The concept of diffusion strengthening refers to the obstruction of diffuse ultrafine particles against internal dislocations in the metal to increase the strength and hardness of the alloying material, resulting in a limited decrease in plasticity and toughness. The greater the number of diffuse phases, the higher the strength of the alloy. The microhardness of gravity cast ER5356 (0.15% Mn), as shown in Figure 9.

In Figure 9, the microhardness values of the extruded rods were gradually increased when they were drawn to the diameters of 9.5 mm, 7.2 mm, 4.6 mm, and 2.0 mm, and the microhardness values were especially maximized at the diameter of 2.0 mm. In addition, the microhardness values were significantly different between semi-continuous casting ER5356 (0.15% Mn) and ER5356 (0.05% Mn), with the former being significantly higher than the latter. In welding ER5356 alloy, the filler wires with 0.05% Mn and 0.15% Mn showed significant differences in forming quality and metal deposition. Joints welded with ER5356 (0.15% Mn) demonstrated superior forming qualities, indicating that the increase in manganese content has a positive effect on the consistency and aesthetics of the weld formation. At a welding current of 125A, ER5356 (0.15% Mn) produced more uniform and aesthetically pleasing weld shapes compared to ER5356 (0.05% Mn) at lower currents, which had irregularly shaped welds and uneven deposition. This highlights the significance of manganese content in achieving high-quality welds with consistent metal deposition patterns and good forming characteristics. However, the microhardness values of gravity cast ER5356 (0.15% Mn) lie between the former two. It is important to note the differences in mechanical properties between semi-continuously cast and gravity cast samples of ER5356 (0.15% Mn). The semi-continuous casting process resulted in improved mechanical performance compared to gravity cast samples. Specifically, semi-continuously cast samples exhibited a 3.17% increase in tensile strength and a 12.8% increase in yield strength. These improvements can be attributed to the refining effect of semi-continuous casting on the microstructure. This includes a more uniform distribution and finer size of Mn-containing phases, which leads to improved resistance to dislocation movement and overall strength of the alloy.

4.2 Comparison of properties of ER5356-WS welded joint organizations incorporated with Mn

In complex application environments, a single alloying element is insufficient to meet performance requirements. Therefore, this study compares the properties of joints produced using ER5356 filler rods with varying Mn contents in section 3.2. The aim is to optimize alloy properties by exploring the influence of additional elements on the properties of ER5356-WS welded joints. Figure 10 displays the microhardness profiles of the 6,082 welded joints produced using various weld currents.

Hardness profiles of 6,082 aluminum alloy welded joints show that the fusion zone has the highest hardness, which is significantly reduced in the HAZ region, as shown in Figure 10. When the welding current increases, there is no significant change in the width of the fusion zone, while the width of the HAZ increases slightly. Manganese content of 0.15% of the wire to get the joint HAZ width is slightly larger than the ER5356 (0.05% Mn) joints. The width of the HAZ is a critical factor in welding as it directly impacts the joint's mechanical properties, such as toughness and fatigue resistance. A wider HAZ can signify excessive heat input, which may result in over-tempered zones and potentially lead to decreased strength and increased brittleness. Therefore, controlling the width of the HAZ is crucial for ensuring the quality and durability of the weld. An increase in manganese concentration, specifically to 0.15% in ER5356 welding wire, has been observed to correspond with a slight increase in HAZ width as compared to the wire containing 0.05% Mn. This effect can be attributed to the influence of manganese on the thermal conductivity and diffusivity of the alloy. Higher manganese content slightly retards the heat dissipation during welding, resulting in a marginally wider HAZ. The relationship between HAZ width and Mn content is a crucial

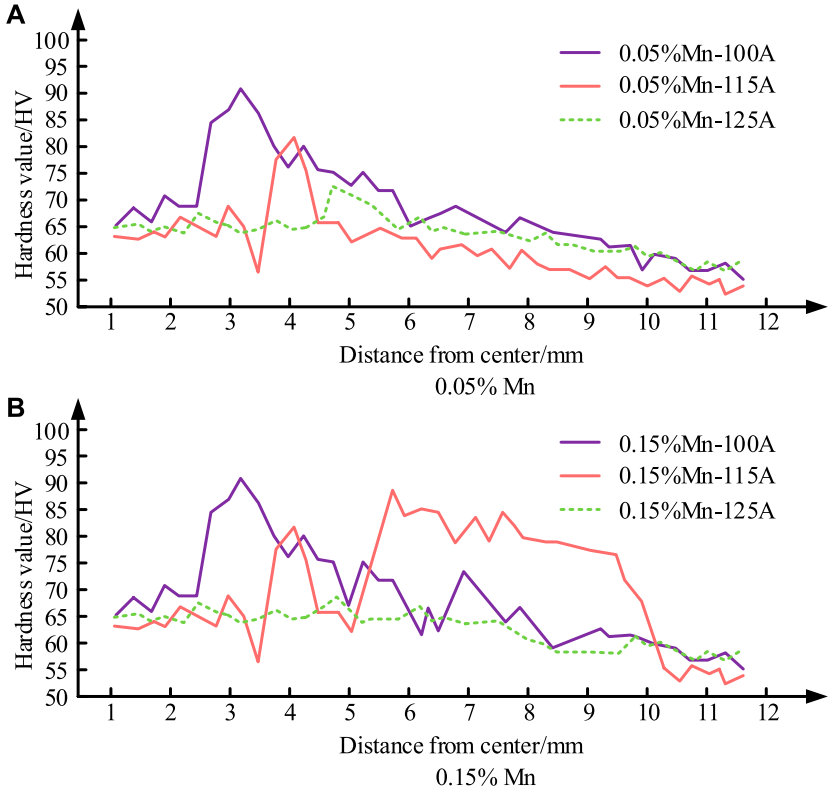

FIGURE 10
Microhardness distribution of 6,082 aluminum alloy welded joints. **(A)** 0.05% Mn. **(B)** 0.15% Mn.

factor to consider when determining welding process parameters. It may be necessary to adjust welding speed or cooling rates to maintain weld integrity and compensate for any differences. Under the condition of lower welding current, there are obvious welding defects in the joints, and the microhardness change has no obvious regularity. However, with the increase of welding current, the regularity of the joint microhardness curve is gradually clear. The results prove that the Mn element can promote the metal deposition process of welding. The macroscopic morphology of 7,005 welded joints, as shown in Figure 11.

In Figure 11, at lower welding current conditions, the weld formation is irregular and the melt deposition is not uniform. However, with the increase of welding current, the quality of weld formation improved. At the same time, the welded joints obtained by ER5356 (0.15% Mn) welding have better forming quality than those obtained by ER5356 (0.05% Mn) welding, in which the metal is more uniformly deposited. Especially under the condition of 125A welding current, the welded joints obtained by ER5356 (0.15% Mn) are more beautifully shaped. 7,005 aluminum alloy welded joints fracture morphology, as shown in Figure 12.

In Figure 12, the welded joint's fracture exhibits ductile fracture, and as the welding current increases, the fracture toughness nest enlarges, and the depth reduces. At 125A welding current, certain areas of the ER5356 (0.05% Mn) wire specimen's joints manifest brittle fracture. The joints joined using ER5356 (0.05% Mn) wire with 125A welding current are at risk of brittle fracture. 15% Manganese (Mn) wire exhibits Mn-rich phases in fracture morphology. This is due to the formation of Al-Mn phases resulting from the Mn element in the 7,005 Aluminum alloy which forms an Al-Mn phase. This not only refines the recrystallized grains, but also dissolves impurity iron and forms an Al (Fe, Mn) phase that reduces the harmful effects of iron and improves the mechanical properties of welded joints. At lower welding currents, an unwelded area is present in the fracture zone. Gradually increasing the welding current reduces this effect. The phenomenon of unwelded joints is particularly mitigated under 125A welding current conditions with ER5356 (0.15% Mn) wire. To investigate the impact of welding current and manganese content on weld shape and deposition, a range of experiments were conducted using different welding currents. The research revealed that lower welding currents result in inadequate fluidity of the melt pool, leading to irregular weld formation and inconsistent metal deposition. This highlights the significant dependence of the welding process on the heat input, which is directly affected by the welding current. As welding current increases, heat input also increases, resulting in improved metal flow and a more stable melt pool. This leads to better weld shape and uniform deposition. Additionally, higher Mn content, such as the Mn content found in ER5356 (0.15% Mn), promotes the formation of fine Mn-containing intermetallic phases and helps stabilize the melt pool under increased welding current. These phases serve as nucleation sites during the solidification process, promoting the formation of finer and more uniform grain structures in the welded metal. The welding current and manganese content have a synergistic effect, resulting in excellent welding outcomes. At 125A, the advantageous effect of higher Mn content becomes

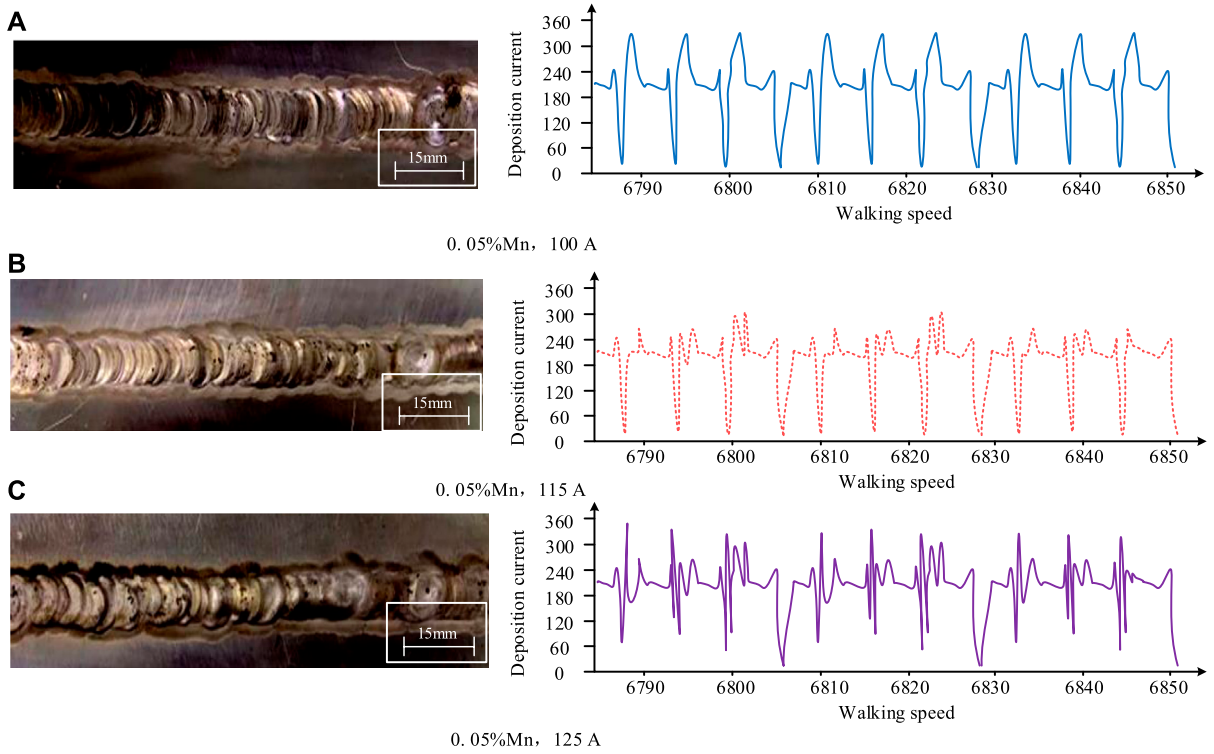

FIGURE 11
Macro morphology of 7,005 welding joint. **(A)** 0.05%Mn, 100 A. **(B)** 0.05%Mn, 115 A. **(C)** 0.05%Mn, 125 A

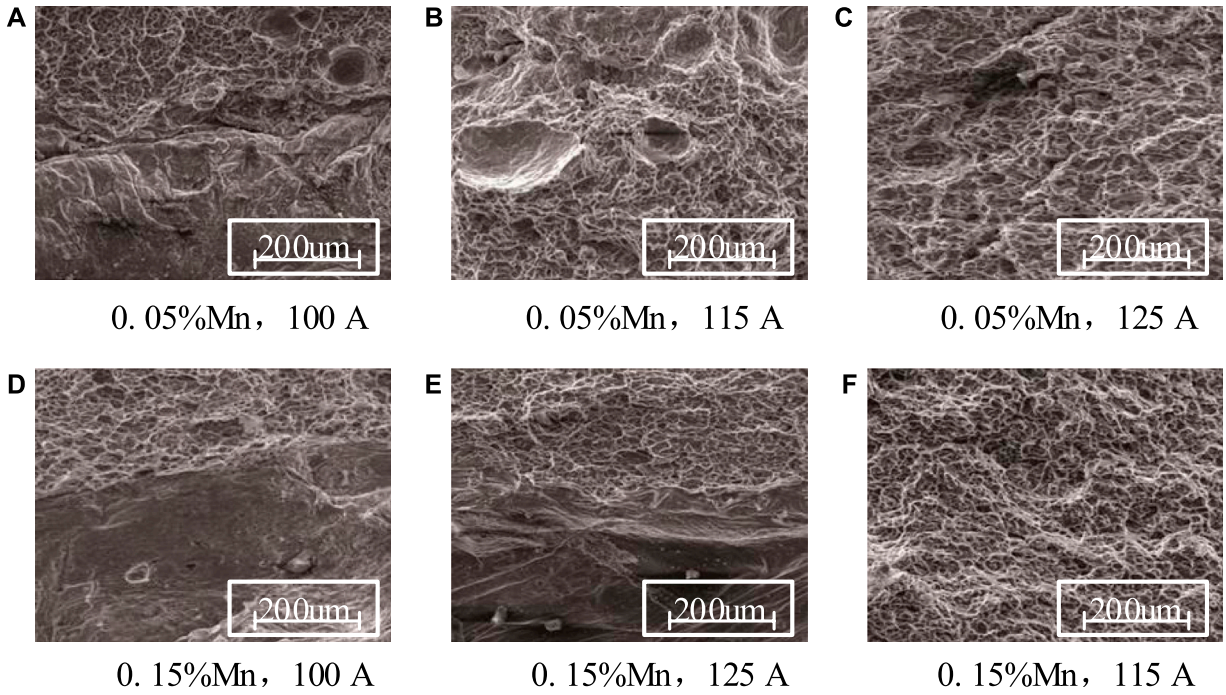

FIGURE 12
Fracture morphology of 7,005 aluminum alloy welded joint. **(A)** 0.05%Mn, 100 A. **(B)** 0.05%Mn, 115 A **(C)** 0.05%Mn, 125 A **(D)** 0.15%Mn, 100 A **(E)** 0.15% Mn, 125 A **(F)** 0.15%Mn, 115 A.

particularly evident, and the shape and uniformity of weld deposition are significantly improved.

This study has practical significance for welding current control, welding quality, and overall mechanical properties of welding. Research has shown that incorporating Mn into ER5356-WS strengthens the metal deposition process and improves the microhardness of the weld seam, particularly when using welding wires with higher Mn content. Therefore, an effective welding current control strategy requires a correct balance between current intensity and welding speed to achieve optimal fusion and mechanical characteristics. Additionally, higher Mn content leads to significantly improved welding quality, fewer welding defects, and a more uniform distribution of microhardness. Therefore, manganese plays a crucial role in achieving excellent welding quality and a better balance between strength and ductility. These findings ultimately contribute to the overall mechanical properties of welds, providing guidance for tailored welding practices that can leverage the advantages of adding Mn to ER5356 to achieve higher tensile and yield strength, and improve toughness.

5 Conclusion

ER5356-WS, which includes manganese, can affect the mechanical properties and weldability of rods during the welding procedure, making it crucial to optimize the welding process. Microhardness testing was conducted on extruded rods with varying diameters to examine the role of manganese in the welding process and its impact on the mechanical properties of the welded joints. The fracture morphology of welded joints produced using different welding currents was also investigated. The study analyzed the influence of manganese (Mn) content in ER5356 welding rod on the mechanical properties and wire structure of aluminum alloy joints. The effects of different Mn contents of ER5356 welding rods (0.05% and 0.15%) on joint performance were compared and analyzed using microhardness analysis, fracture morphology observation, and tensile strength testing. The study found that samples cast with ER5356 welding rod containing 0.15% Mn exhibited a 12.8% increase in yield strength and a 3.17% increase in tensile strength compared to traditional gravity casting. Additionally, the joint formed by welding rods containing 0.15% Mn had a wider HAZ than the joint formed by welding rods containing 0.05% Mn. It was also observed that lower welding currents resulted in irregularly shaped weld seams with uneven deposition characteristics. When a welding current of 125A was used, brittle fracture may occur in certain areas of the joint of the electrode sample containing 0.05% Mn. These findings demonstrated the important role of the Mn element in the welding process and provide guidance for improving welding current control, welding quality. This research emphasizes the significance of manganese in the welding procedure, serving as a useful resource for optimizing it. Although the role of manganese in the welding procedure is now clearer, additional research is necessary to explore other factors that could impact the MP and WWS of welded strips. This will facilitate the optimization of welding procedures.

Data availability statement

The original contributions presented in the study are included in the article/Supplementary Material, further inquiries can be directed to the corresponding author.

Author contributions

XN: Conceptualization, Writing–original draft. SX: Methodology, Writing–original draft. HM: Writing–review and editing.

Funding

The author(s) declare that no financial support was received for the research, authorship, and/or publication of this article.

Conflict of interest

The authors declare that the research was conducted in the absence of any commercial or financial relationships that could be construed as a potential conflict of interest.

Publisher's note

References

Abhijit, A., Varghese, J., Chalavadi, P., He, T., Feng, M., and Rajulapati, K. V. (2019). Negative strain rate sensitivity in two-phase nanocrystalline CoCrFeMnNi high-entropy alloy with broader grain size distribution studied by nanoindentation. *Trans. Indian Inst. Metals* 72 (10), 2861–2867. doi:10.1007/s12666-019-01762-5

Ahmed, M. M. Z., El-Sayed Seleman, M. M., Fydrych, D., and Cam, G. (2023a). Review on friction stir welding of dissimilar magnesium and aluminum alloys: scientometric analysis and strategies for achieving high-quality joints. *J. Magnesium Alloys* 11 (11), 4082–4127. doi:10.1016/j.jma.2023.09.039

Ahmed, M. M. Z., El-Sayed Seleman, M. M., Fydrych, D., Fydrych, D., and Çam, G. (2023b). Friction stir welding of aluminum in the aerospace industry: the current progress and state-of-the-art review. *Materials* 16 (8), 1–11. doi:10.3390/ma16082971

Baskoro, A. S., Milyardi, I., and Amat, M. A. (2020). The effect of welding parameter on mechanical properties and macrostructure of AA1100 using autogenous TIG welding. *Int. J. Automot. Mech. Eng.* 17 (1), 7562–7569. doi:10.15282/ijame.17.1.2020.05.0560

Cam, G., and Ipekoglu, G. (2017). Recent developments in joining of aluminum alloys. *Int. J. Adv. Manuf. Technol.* 91 (5-8), 1851–1866. doi:10.1007/s00170-016-9861-0

Cam, G., Javaheri, V., and Heidarzadeh, A. (2023). Advances in FSW and FSSW of dissimilar Al-alloy plates. *J. Adhesion Sci. Technol.* 37 (2), 162–194. doi:10.1080/01694243.2022.2028073

Çömez, N., and Durmuş, H. (2020). Corrosion behavior and mechanical properties of cold metal transfer welded dissimilar AA7075-AA5754 alloys. *J. Central South Univ.* 27 (1), 18–26. doi:10.1007/s11771-020-4274-5

Fang, Y., Luo, B., Zhao, T., He, D., Jiang, B., and LiuST-Sigma, Q. (2022). ST-SIGMA: spatio-temporal semantics and interaction graph aggregation for multi-agent perception and trajectory forecasting. *CAAI Trans. Intell. Technol.* 7 (4), 744–757. doi:10.1049/cit2.12145

Haryadi, G. D., Dewa, R. T., Ekaputra, I. M. W., and Suprihanto, A. (2020). Investigation of post-weld heat treatment (T6) and welding orientation on the strength of TIG-welded AL6061. *Open Eng.* 10 (1), 753–761. doi:10.1515/eng-2020-0084

Ipekoglu, G., and Cam, G. (2019). Formation of weld defects in cold metal transfer arc welded 7075-T6 plates and its effect on joint performance. *IOP Conf. Ser. Mater. Sci. Eng.* 629 (1), 012007–012012. doi:10.1088/1757-899x/629/1/012007

Kashaev, N., Ventzke, V., and Cam, G. (2018). Prospects of laser beam welding and friction stir welding processes for aluminum airframe structural applications. *J. Manuf. Process.* 36 (12), 571–600. doi:10.1016/j.jmapro.2018.10.005

Khaliq, U. A., Yusof, F., Chen, Z., Mohd Isa, M. S., Cam, G., et al. (2023). A review on friction stir butt welding of aluminum with magnesium: a new insight on joining mechanisms by interfacial enhancement. *J. Mater. Res. Technol.* 27, 4595–4624. doi:10.1016/j.jmrt.2023.10.158

Khan, M., Dewan, M. W., and Sarkar, M. Z. (2021). Effects of welding technique, filler metal and post-weld heat treatment on stainless steel and mild steel dissimilar welding joint. *Journal of Manufacturing Processes* 64 (268), 1307–1321. doi:10.1016/j.jmapro.2021.02.058

Kim, G. G., Kim, D. Y., Hwang, I., Kim, D., Kim, Y. M., and Park, J. (2021). Mechanical properties of aluminum 5083 alloy GMA welds with different magnesium and manganese content of filler wires. *Appl. Sci.* 11 (24), 11655–11714. doi:10.3390/app112411655

Kim, G. W., Jeong, S. M., and Song, K. H. (2023). Microstructure and mechanical properties of dissimilar friction-welded commercially pure Ti and Ti-6Al-4V alloy. *Materials Transactions* 64 (6), 1257–1264. doi:10.2320/matertrans.MT-MI2022001

Kucukomeroglu, T., Aktarer, S. M., Ipekoglu, G., and Cam, G. (2019). Investigation of mechanical and microstructural properties of friction stir welded dual phase (DP) steel. *IOP Conf. Ser. Mater. Sci. Eng.* 629 (5), 012010–012012. doi:10.1088/1757-899x/629/1/012010

Mehdi, H., and Mishra, R. S. (2020). Influence of friction stir processing on weld temperature distribution and mechanical properties of TIG-welded joint of AA6061 and AA7075. *Trans. Indian Inst. Metals* 73 (7), 1773–1788. doi:10.1007/s12666-020-01994-w

Mercan, E., Ayan, Y., and Kahraman, N. (2020). Investigation on joint properties of AA5754 and AA6013 dissimilar aluminum alloys welded using automatic GMAW. *Eng. Sci. Technol. Int. J.* 23 (4), 723–731. doi:10.1016/j.jestch.2019.11.004

Nafeez, A. L., Veeman, D., and Muthu, S. M. (2022). Effect of addition of scandium in filler rod on tungsten inert gas welding of AA5052-H32 alloy. *Russ. J. Non-Ferrous Metals* 63 (3), 315–327. doi:10.3103/s1067821222030099

Naing, T. H., and Muangjunburee, P. (2022). Metallurgical and mechanical characterization of MIG welded repair joints for 6082-T6 aluminum alloy with ER 4043 and ER 5356. *Trans. Indian Inst. Metals* 75 (6), 1583–1593. doi:10.1007/s12666-022-02523-7

Peng, P., She, J., Tang, A., Zhang, J., Song, K., Yang, Q., et al. (2022). A strategy to regulate the microstructure and properties of Mg-2.0 Zn-1.5 Mn magnesium alloy by tracing the existence of Mn element. *J. Alloys Compd.* 890 (1), 161789–161794. doi:10.1016/j.jallcom.2021.161789

Qi, Y., He, T., and Feng, M. (2021). The effect of Cu and Mn elements on the mechanical properties of single-crystal CoCrFeNi-based high-entropy alloy under nanoindentation. *J. Appl. Phys.* 129 (19), 195104–195110. doi:10.1063/5.0043034

Qu, Z., Han, T., Cui, H., and Tang, X. (2021). A comparison between Tungsten inert Gas welded joints welded by Commercial ER5183 filler and Al–Mg–Zn–Sc–Zr–Mn filler on microstructure and properties in 7075-T651 aluminum alloys. *Mater. Trans.* 62 (3), 386–395. doi:10.2320/matertrans.mt-m2020295

Salah, A. N., Mabuwa, S., Mehdi, H., Msomi, V., Kaddami, M., and Mohapatra, P. (2022). Effect of multipass FSP on Si-rich TIG welded joint of dissimilar aluminum alloys AA8011-H14 and AA5083-H321: EBSD and microstructural evolutions. *Silicon* 14 (15), 9925–9941. doi:10.1007/s12633-022-01717-4

Samiuddin, M., Li, J., Taimoor, M., Siddiqui, M. N., Siddiqui, S. U., and Xiong, J. T. (2021). Investigation on the process parameters of TIG-welded aluminum alloy through mechanical and microstructural characterization. *Def. Technol.* 17 (4), 1234–1248. doi:10.1016/j.dt.2020.06.012

Senol, M., and Cam, G. (2023). Investigation into microstructures and properties of AISI 430 ferritic steel butt joints fabricated by GMAW. *Int. J. Press. Vessels Pip.* 202 (4), 104926–105012. doi:10.1016/j.ijpvp.2023.104926

Senthur Vaishnavan, S., and Jayakumar, K. (2021). Performance analysis of TIG welded dissimilar aluminium alloy with scandium added ER5356 filler rods. *J. Chin. Inst. Eng.* 44 (7), 718–725. doi:10.1080/02533839.2021.1940298

Serindag, H. T., and Cam, G. (2023). Characterizations of microstructure and properties of dissimilar AISI 316l/9Ni low-alloy cryogenic steel joints fabricated by gas tungsten arc welding. *J. Mater. Eng. Perform.* 32 (3), 7039–7049. doi:10.1007/s11665-022-07601-x

Serindag, H. T., Tardu, C., Kircicek, I. O., and Cam, G. (2022). A study on microstructural and mechanical properties of gas tungsten arc welded thick cryogenic 9% Ni alloy steel butt joint. *CIRP J. Manuf. Sci. Technol.* 37, 1–10. doi:10.1016/j.cirpj.2021.12.006

Sokoluk, M., Cao, C., Pan, S., and Li, X. (2019). Nanoparticle-enabled phase control for arc welding of unweldable aluminum alloy 7075. *Nat. Commun.* 10 (1), 98–106. doi:10.1038/s41467-018-07989-y

Waziri, T. A., and Ibrahim, A. (2022). Discrete fix up limit model of a device unit. *J. Comput. Cognitive Eng.* 2 (2), 163–167. doi:10.47852/bonviewjcce2202166

Yılmaz, E., and Fındık, F. (2022). Effect of shielding gas on microstructure and mechanical properties in AA6061-T6 alloy MIG welding. *Periodicals Eng. Nat. Sci.* 10 (1), 268–277. doi:10.21533/pen.v10i1.2159